C. R. Mecanique 340 (2012) 829–844

Contents lists available at SciVerse ScienceDirect

Comptes Rendus Mecanique

www.sciencedirect.com

Out of Equilibrium Dynamics

Initiation of reactive blast waves by external energy sources

Amable Liñán [a,*], Vadim N. Kurdyumov [b], Antonio L. Sánchez [c]

[a] ETSI Aeronáuticos, Universidad Politécnica de Madrid, 28040 Madrid, Spain
[b] Departamento de Energía, CIEMAT, 28040 Madrid, Spain
[c] Grupo de Mecánica de Fluidos, Universidad Carlos III de Madrid, 28911 Leganés, Spain

ARTICLE INFO

Article history:
Available online 13 November 2012

Keywords:
Fast-reacting detonation
Detonation initiation
Self-sustained detonations
Initiation energy of detonations
Reacting blast waves

ABSTRACT

This article is devoted to the analysis of the direct initiation, by concentrated centrally-symmetric external energy sources, of self-sustained detonation waves in gaseous reactive mixtures. The dynamics of the detonation front will be described in the fast reaction limit, when the thickness of the reaction layer that follows the shock front is very small compared with the shock radius. At early times, after starting the external thermal energy deposition, the detonation front, associated with a strongly expanding flow, is overdriven; thus it is reached by expansion waves that decrease its velocity towards the Chapman–Jouguet (CJ) value, for which the expansion waves can no longer reach the front. The decay occurs for detonation radii such that the energy released by the external source equals the heat released by the chemical reaction. For planar detonations the CJ velocity is only approached asymptotically for large times, while for cylindrical and spherical detonations the flow divergence provides an additional decay mechanism associated with the front curvature that causes the transition to the constant CJ velocity to occur at a finite value of the detonation radius. The time evolution of the flow field and the corresponding variation with deposition time of the transition radius is computed for energy sources of constant heating rate. The analysis includes a detailed quantitative description of the near-front flow structure for times close to the transition time, given here for the first time, along with the study of the evolution towards the Zel'dovich–Taylor cylindrical or spherical self-similar flow structure, which corresponds to a CJ detonation front ideally initiated at the center without any external energy source. The asymptotic decay to CJ is also described for planar detonations initiated with energy sources of constant heating rate and finite nonzero deposition time. A brief discussion will be given on how the reaction may be quenched by the flow divergence effects if the initiating energy is smaller than a critical value, thus failing to generate a self-propagating detonation wave.

1. Introduction

We shall show below how an external source of thermal energy in a reactive gaseous medium, when spatially concentrated and with a small deposition time, initiates a detonation front that propagates with supersonic speeds in the medium. This is so because of the high temperature sensitivity of the chemical reactions, which are frozen at the initial low temperatures, but become very fast when the reactive mixture is heated by the shock wave generated by the thermal energy source at early times. Thus the chemical reactions occur rapidly behind the shock front and are therefore completed in a thin layer, which, together with the much thinner shock, forms the detonation front. The heat release due to the reactions

* Corresponding author.
E-mail addresses: amable.linan@upm.es (A. Liñán), vadim.k@ciemat.es (V.N. Kurdyumov), asanchez@ing.uc3m.es (A.L. Sánchez).

1631-0721/$ – see front matter
http://dx.doi.org/10.1016/j.crme.2012.10.033

contribute to sustain the detonation, which will become self-sustained if the reaction layer remains sufficiently thin during the first overdriven stage.

The internal structure of the detonation front, whose thickness is much smaller than the shock radius, is quasi-planar and quasi-steady in the first approximation. Zel'dovich [1], Neumann [2], and Döring [3] described independently in the early 1940's the planar and steady internal detonation structure as a nonreactive shock wave followed by a non-viscous diffusionless reactive layer. This quasi-steady and quasi-planar ZND analysis, which is used in the following to calculate the jump conditions at the detonation front, is based on the small value of the fraction of molecular collisions that lead to a chemical reaction.

The detonation front separates the chemically-frozen outer gas mixture, which is typically stagnant and spatially uniform, from the reacted gas, whose motion, initially started by the external heat release, is sustained at later stages by the release of heat due to the reaction. The velocities associated with the motion of the reactive gases are of the order of the local sound velocity behind the detonation front; so that the corresponding Reynolds numbers are very large and the flow behind the detonation is inviscid, outside a hot core of nearly uniform pressure created, as we shall see, by the external concentrated heat addition.

The infinitely fast reaction limit (called by Korobeinikov [4] "detonation-wave model"), in which the reactive front is treated as a discontinuity, is applicable to the description of reactive blast waves when the thickness of the reaction layer is small compared with the detonation radius $r'_d(t')$, an increasing function of the time t'. The flow is described by the Euler equations for the density ρ', pressure p' and radial velocity v'. The outer boundary conditions are given by the values of the flow variables, $\rho' = \rho'_d$, $p' = p'_d$ and $v' = v'_d$, immediately behind the detonation front, at $r' = r'_d$. These values are determined in terms of the ambient properties $\rho' = \rho'_o$, $p' = p'_o$ and $v' = 0$ by the Rankine–Hugoniot jump conditions of conservation of mass, momentum and energy $\rho'_o D' = \rho'_d(D' - v'_d)$, $p'_o + \rho'_o D'^2 = p'_d + \rho'_d(D' - v'_d)^2$, and $h'_o + q_R + D'^2/2 = \gamma/(\gamma-1)(p'_d/\rho'_d) + (D' - v'_d)^2/2$. In writing the energy equation we have assumed that the reacted gas behaves as a perfect gas with a constant value γ of the ratio of the specific heats. In the formulation, $D' = \mathrm{d}r'_d/\mathrm{d}t'$ is the detonation velocity, h'_o is the ambient thermal enthalpy, and q_R is the amount of heat released by the reaction per unit mass of gas mixture. Typical detonations propagate at large Mach numbers, that is, with propagation velocities much larger than the ambient sound velocity. Then, the ambient pressure p'_o is found to be smaller than the momentum flux $\rho'_o D'^2$ by a factor of order of the square of the propagation Mach number, and shall be consequently neglected in the momentum jump condition. Note that, in this strong-shock approximation, one could in principle neglect also the initial thermal enthalpy h'_o in the energy balance equation, but the errors in evaluating the temperature associated with this additional simplification are found to be more important, when computing the reaction rates, than those involved in neglecting the effect of the ambient pressure; so that for increased accuracy, when evaluating the temperature behind the shock, we choose to retain this relatively small term in the analysis.

Detonations can be initiated directly by releasing an amount of energy E at a concentrated location (e.g., explosive charge), along a line (e.g., electric spark, laser beam), or at a plane, which generates a strong overdriven detonation bounding a region of rapidly expanding radial motion of the burnt gases. The expansion waves propagating from the central nearly empty region reach the detonation front and continuously weaken it. If the detonation propagation velocity decreases to reach the Chapman–Jouguet (CJ) value, defined by the condition that the gas velocity relative to the front just behind the detonation, $u'_d = D' - v'_d$, is equal to the local value of the sound velocity, $a'_d = (\gamma p'_d/\rho'_d)^{1/2}$, then the expansion waves can no longer reach the front. Afterwards, the front propagation will be self-sustained.

There are numerous numerical studies, incorporating finite-rate effects, of the transition to the self-propagating mode of detonation. They show that the transition involves oscillations of the shock front and its accompanying reaction layer, and that only for initiation energies above a critical value this transition is possible. However, these numerical studies do not provide a sufficiently clear physical understanding of why the critical initiation energy turns out to be several orders of magnitude larger than that predicted by the criterion put forward by Zel'dovich et al. [5], namely, that the initiation energy should be large enough to ensure that the detonation radius at transition r'_c be larger than the thickness of the reaction layer. In 1994, He and Clavin [6] carried out a quasi-steady analysis of the structure of the reaction layer behind the shock front, propagating with the CJ velocity. Their analysis incorporates the effects of the radius of curvature of the front, leading to a critical value r'_d below which no quasi-steady solution exists. For a one-step irreversible reaction with Arrhenius kinetics with large activation energy the resulting value is

$$\frac{(r'_d)^*}{l_i} = \frac{8e\gamma^2 j}{\gamma^2 - 1}\beta \tag{1}$$

where β represents the nondimensional activation energy based on the Newmann temperature behind the shock wave and l_i is the associated induction length. The condition that the detonation radius at transition to CJ, which is a function of the energy released by the external source E, be larger than the critical radius r'_d provides then a natural initiation criterion, with critical conditions obtained by equating both radii. In their analysis, He and Clavin used the decay law for the nonreactive point-explosion blast wave of Sedov [7] and Taylor [8] to deduce an approximate value for the detonation radius at transition, with resulting values of the critical initiation energy E_c in reasonably good agreement with direct numerical simulations and experimental observations [6].

The sonic condition $D'_d - v'_d = a'_d$ together with the Rankine–Hugoniot jump equations, written with the strong-shock approximation, lead to

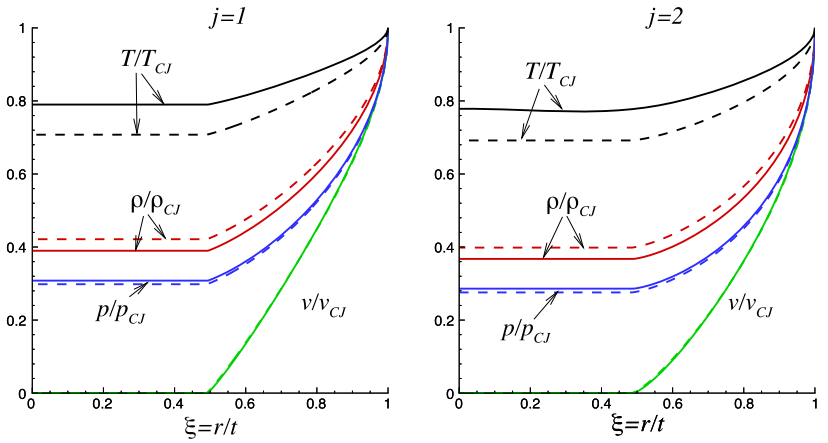

Fig. 1. Cylindrical ($j=1$) and spherical ($j=2$) ZT solutions for $\gamma=1.4$ (dashed curves) and $\gamma=1.25$ (solid curves), the latter being a value more typical of detonation products.

$$\frac{a'_{\mathrm{CJ}}}{D'_{\mathrm{CJ}}}=\frac{D'_{\mathrm{CJ}}-v'_{\mathrm{CJ}}}{D'_{\mathrm{CJ}}}=\frac{\rho'_o}{\rho'_{\mathrm{CJ}}}=\frac{\gamma}{\gamma+1} \tag{2}$$

and

$$\frac{p'_{\mathrm{CJ}}}{\rho'_o(D'_{\mathrm{CJ}})^2}=\frac{1}{\gamma+1} \tag{3}$$

for the values a'_{CJ}, v'_{CJ}, ρ'_{CJ}, and p'_{CJ} behind the CJ detonation, along with the corresponding propagation velocity

$$\left(D'_{\mathrm{CJ}}\right)^2/2=\left(\gamma^2-1\right)\left(q_R+h'_o\right) \tag{4}$$

Zel'dovich [9] and Taylor [10] independently described the self-similar flow structure, with central symmetry, behind a constant-velocity CJ detonation front originating, ideally, at the center without an external initiating energy. In the absence of geometrical scales, the flow must be self-similar with the similarity variable $\xi=r'/(D'_{\mathrm{CJ}}t')$. The Zel'dovich–Taylor (ZT) solution of the nonreacting Euler equations, determined by the CJ jump conditions at $\xi=1$, includes an outer shell of outward moving gas and a core of stagnant gas with uniform properties, separated by a weak discontinuity at $\xi=\xi_o^+$, where $v'=0$. Since the detonation front moves at constant velocity, the flow is homentropic, so that

$$\left(\frac{p'}{p'_{\mathrm{CJ}}}\right)^{(\gamma-1)/\gamma}=\left(\frac{\rho'}{\rho'_{\mathrm{CJ}}}\right)^{\gamma-1}=\left(\frac{a'}{a'_{\mathrm{CJ}}}\right)^2 \tag{5}$$

For the planar case, $\xi_o^+=1/2$, and the solution is given by (5) and

$$\frac{v'}{D'_{\mathrm{CJ}}}=\frac{2a'/D'_{\mathrm{CJ}}-1}{\gamma-1}=\frac{2\xi-1}{\gamma+1} \tag{6}$$

for $1/2<\xi<1$ and $v'=a'-D'_{\mathrm{CJ}}/2=0$ for $0<\xi<1/2$. Numerical integration is required to solve the problem in the cylindrical and spherical cases, the resulting profiles are given in Fig. 1. We shall show below how this ZT solution is reached for large times after the detonation is initiated by a strong enough external thermal-energy source, an essential mechanism for initiation of detonations in unconfined gaseous reactive mixtures.

The characteristic length scale involved in the direct initiation process of CJ detonations for short deposition times, t'_d, can be derived from the propagation velocity, D'_{CJ}, the ambient density ρ'_o, and the total initiating energy, E, by the condition $E=\rho'_o(D'_{\mathrm{CJ}})^2(r'_{\mathrm{E}})^{j+1}$ that the initiating energy E (i.e., energy per unit length in line sources and energy per unit surface in planar sources) be comparable to the energy released by chemical reaction of the gas inside the front. This defines a characteristic length

$$r'_{\mathrm{E}}=\left(\frac{E}{\rho'_o(D'_{\mathrm{CJ}})^2}\right)^{1/(j+1)} \tag{7}$$

and a corresponding characteristic time

$$t'_{\mathrm{E}}=r'_{\mathrm{E}}/D'_{\mathrm{CJ}} \tag{8}$$

with $j = (0, 1, 2)$ used to denote plane, line and point sources, respectively. Here, the heat released per unit mass q_R, in agreement with (4), is taken to be of order $(D'_{\rm CJ})^2$ in the above estimates.

We shall analyze below the initiation of self-sustained blast waves by localized energy sources of characteristic size $r'_s \ll r'_{\rm E}$ with deposition times $t'_d \lesssim t'_{\rm E}$. Concentrated sources were also considered in the previous numerical studies of Bishimov [11] (reported by Korobeinikov[12]), Kyong [13] (discussed in [14]) and Korobeinikov and Markov [15], all of them devoted to the problem of instantaneous heat release corresponding to the limit $t'_d/t'_{\rm E} \to 0$ (see [16] for additional entries into the early literature). The initial conditions for the problem were written for $t' \ll t'_{\rm E}$, when the effect of the chemical heat release is negligible and the solution is that described, independently, by Sedov [7] and Taylor [8] for a strong point explosion. The expansion waves were found to progressively weaken the overdriven detonation causing its velocity D' to decay continuously. As anticipated by Levin and Chernyi [17], for planar detonations the velocity approaches asymptotically the CJ value for $t' \ll t'_{\rm E}$, whereas for spherical and cylindrical detonations the CJ velocity is reached at a finite critical time t'_c when $r'_d = r'_c \sim r'_{\rm E}$. As pointed out in [12], the computation "becomes very complex due to the presence of peculiar conditions on the shock wave front as it nears the CJ point". The complex structure of the near-front solution at transition to CJ, conjectured in the analytical work [17] (see also the discussion given in [18]), has hindered in the past the numerical computation of the flow, in the infinite-reaction-rate limit, for $t' \geqslant t'_c$. For instance, the previous numerical calculations either end before $t' = t'_c$ [11,12] or fail to reproduce the near-front solution for $t' \geqslant t'_c$ [13,14], in that their computations do not reproduce the infinite gradients that appear behind the CJ front. Korobeinikov and Markov [15] succeeded in computing the values of t'_c and r'_c for different values of γ in spherical and cylindrical geometries, but given the resolution of their figures it is unclear whether their post-transition profiles were satisfactorily reproduced.

It will be shown below that the combined effects of the expansion waves reaching the initially overdriven detonation and of the flow divergence are responsible for the continuous deceleration of the detonation for $t' < t'_c$, with the latter being dominant in the final stages of the detonation transition to CJ. For $t' > t'_c$ the expansion waves can no longer reach the CJ detonation and the three characteristics of the Euler equations will be seen to leave from the front towards the burnt gases. The last outward-running characteristic that reaches the front is tangent to the detonation trajectory at $t' = t'_c$. For $t' > t'_c$, this critical characteristic is left behind the front, defining the inner boundary of a self-propagating shell that extends between this characteristic and the CJ detonation. The solution in this shell, independent of that found inside the critical characteristic, corresponds, exactly, to the ZT solution discussed above.

Understanding the changes in the pattern of characteristics occurring at $t' = t'_c$ will enable the numerical integration to be extended for $t' \geqslant t'_c$, including the accurate description of the self-propagating shell. Unlike the previous computations [12, 14,15], our calculations consider point and line energy sources of finite deposition time, $t'_d \sim t'_c$, to determine the variation of $r_c = r'_c/r'_{\rm E}$ and $t_c = t'_c/t'_{\rm E}$ with $t_d = t'_d/t'_{\rm E}$, including as a limiting case the instantaneous heat deposition analyzed previously in the literature. Also, the near-front structure at transition is investigated in terms of a Burgers-like universal equation accounting for curvature effects. The planar solution is also addressed for sources of constant heating rate, including the evolution for large times and the analytical description of the flow when the initially detonation is marginally overdriven.

Note that the analysis given here finds applicability in connection with Clavin's previous work [6]. According to the initiation criterion proposed in [6], for a successful initiation, when the CJ solution is reached the detonation-front radius r'_c must be larger than the critical radius associated with the solution of the steady curved reaction front, given in (1). Therefore, the values of $r_c = r'_c/r'_{\rm E}$ computed below can be directly applied, together with Clavin's criterion $r'_c = r'_d$, to provide a quantitative prediction for the minimum initiation energy according to

$$E_c = \rho'_o D'^2_{\rm CJ} \left(\frac{\beta l'_i}{r_{\rm CJ}}\right)^{1+j} \left(\frac{8ej\gamma^2}{\gamma^2-1}\right)^{1+j} \tag{9}$$

Also, the study of the near-front structure at transition can be used as a basis to enable future analyses of the critical initiation conditions based on finite-rate studies of the inner detonation structure, extending Paul Clavin's [6] work by including unsteady effects.

2. Formulation

As previously mentioned, the flow of the reacted gases behind the detonation is effectively inviscid. In writing the Euler equations for a perfect gas with constant specific-heat ratio γ

$$\frac{\partial \rho}{\partial t} + \frac{\partial}{\partial r}(\rho v) + \frac{j\rho v}{r} = 0 \tag{10}$$

$$\frac{\partial v}{\partial t} + v\frac{\partial v}{\partial r} + \frac{1}{\rho}\frac{\partial p}{\partial r} = 0 \tag{11}$$

$$\frac{\partial}{\partial t}\left(p/\rho^\gamma\right) + v\frac{\partial}{\partial r}\left(p/\rho^\gamma\right) = 0 \tag{12}$$

the time and radial distance are scaled with $t'_{\rm E}$ and $r'_{\rm E}$, respectively, giving the dimensionless coordinates $r = r'/r'_{\rm E}$ and $t = t'/t'_{\rm E}$ together with the detonation propagation velocity $D = D'/D'_{\rm CJ}$, whereas the density, velocity and pressure are

scaled with ρ'_o, D'_{CJ} and $\rho'_o(D'_{CJ})^2$, to give the variables ρ, v and p. Planar, cylindrical and spherical geometries correspond to $j=0$, $j=1$ and $j=2$, respectively. Note that, for computational purposes, it is often convenient to write the Euler equations (10)–(12) in their characteristic form

$$\frac{\partial}{\partial t}\left(v+\frac{2}{\gamma-1}a\right)+(v+a)\frac{\partial}{\partial r}\left(v+\frac{2}{\gamma-1}a\right)-\frac{a^2}{\gamma(\gamma-1)}\frac{\partial}{\partial r}\left(\frac{s}{c_v}\right)+\frac{jva}{r}=0 \tag{13}$$

$$\frac{\partial}{\partial t}\left(v-\frac{2}{\gamma-1}a\right)+(v-a)\frac{\partial}{\partial r}\left(v-\frac{2}{\gamma-1}a\right)-\frac{a^2}{\gamma(\gamma-1)}\frac{\partial}{\partial r}\left(\frac{s}{c_v}\right)-\frac{jva}{r}=0 \tag{14}$$

$$\frac{\partial s}{\partial t}+v\frac{\partial s}{\partial r}=0 \tag{15}$$

where $a=(\gamma p/\rho)^{1/2}$ is the sound speed and the ratio of the entropy s to the specific heat at constant volume c_v is given by $s/c_v=\ln(p/\rho^\gamma)$. The first two characteristics C^+ and C^-, moving with velocity $v\pm a$, correspond to acoustic waves, whereas C^0 corresponds to the particle paths, moving with the gas velocity v.

The Rankine–Hugoniot jump conditions determine the boundary conditions

$$r=r_d(t):\quad v-v_d=\rho-\rho_d=p-p_d=0 \tag{16}$$

where the fluid variables can be written, for overdriven waves, in the form

$$\frac{D-v_d}{D}=\frac{1}{\rho_d}=\frac{\gamma}{\gamma+1}-\frac{1}{\gamma+1}\left(1-D^{-2}\right)^{1/2} \tag{17}$$

and

$$p_d=\frac{D^2}{\gamma+1}\left[1+\left(1-D^{-2}\right)^{1/2}\right] \tag{18}$$

in terms of the propagation velocity $D=\mathrm{d}r_d/\mathrm{d}t$. For $D=1$, these expressions reduce to the CJ values

$$\rho_{CJ}=\frac{\gamma+1}{\gamma}\quad\text{and}\quad p_{CJ}=v_{CJ}=\frac{1}{\gamma+1} \tag{19}$$

with the corresponding sound speed being

$$a_{CJ}=\gamma/(\gamma+1) \tag{20}$$

The direct initiation problem addressed here considers the localized deposition of a finite amount of energy E at the origin. For sources with deposition time t'_d much smaller than t'_E, the case considered in previous studies, the external heat release is effectively instantaneous, with the initial solution for $t_d\ll t\ll 1$ corresponding to the nonreactive Sedov–Taylor blast wave, with $t_d=t'_d/t'_E\ll 1$ representing the dimensionless deposition time. For the general case $t'_d\sim t'_E$ considered here (i.e., $t_d\sim O(1)$) the flow associated with the finite-rate heat source must be analyzed when describing the initiation of the self-sustained detonation. As shown by Kurdyumov et al. [19] when analyzing the flow induced by concentrated external heat sources in nonreactive gases, the flow includes a neatly defined core, of radius $r_e(t)\sim r_d(t)$, of very hot expanding gas dominated by heat conduction from the source. The velocities in the core region and in the outer inviscid region are of the same order; however, because of the resulting high temperatures, the local Mach number, although taking values of order unity outside, is very small in the core. The pressure in this hot kernel is uniform in the first approximation, with a value $p_e(t)$ comparable to p_d, whereas the density is much lower. The edge of the resulting almost-empty region appears as a contact surface, so that the condition

$$v=\frac{\mathrm{d}r_e}{\mathrm{d}t}\quad\text{at } r=r_e \tag{21}$$

applies. This contact surface acts as a piston for the outer flow, assisting the motion of the outward propagating detonation. Integrating with respect to r the low Mach number energy equation in the hot core $0<r\leqslant r_e$, dominated by heat conduction from the external energy source at the origin, yields an equation linking the temporal evolution of the contact-surface radius $r_e(t)$ and the hot core pressure p_e. For instance, for the centrally-symmetric cases, the equation can be written as

$$\frac{\mathrm{d}}{\mathrm{d}t}\left(\frac{2^j\pi}{j+1}r_e^{(j+1)}\frac{p_e}{\gamma-1}\right)+2^j\pi r_e^j p_e\frac{\mathrm{d}r_e}{\mathrm{d}t}=q(t) \tag{22}$$

for $j\neq 0$, with the factor π appearing in the left-hand side terms replaced by 2 for the planar case $j=0$. The source heating rate q' is scaled with its characteristic value $E/t'_E=\rho'_o D'^3_{CJ} r'^j_E$ to give the dimensionless heating function q, which

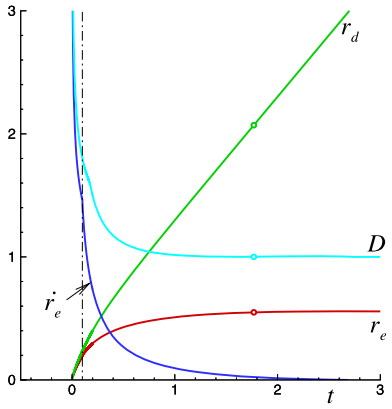

Fig. 2. The evolution with time of r_d, r_e, D and $\dot{r}_e = \mathrm{d}r_e/\mathrm{d}t$ for $t_d = 0.1$, $\gamma = 1.4$ and $j = 1$; the circles mark the transition to CJ detonation.

must therefore satisfy $\int_0^{t_d} q\,\mathrm{d}t = 1$. For instance, for the case of constant heating rate considered in the integrations below one obtains

$$q = 1/t_d \quad \text{for } 0 < t < t_d \quad \text{and} \quad q = 0 \quad \text{for } t > t_d \tag{23}$$

The above equation (22) states that the heat added at the origin is partly employed to increase the internal energy of the hot conductive pocket, and partly transferred to the outer fluid when displacing it with the velocity $\mathrm{d}r_e/\mathrm{d}t$ (note that the internal energy per unit volume, $p_e/(\gamma - 1)$, is written for a constant value of γ). For $t > t_d$ (22) reduces to

$$\frac{\mathrm{d}}{\mathrm{d}t}\left[p_e\left(\frac{2^j\pi}{j+1}r_e^{j+1}\right)^{\gamma}\right] = 0 \tag{24}$$

indicating that the evolution of the inner hot region is globally isentropic in the post-heating period.

The description of initiation of reactive blast waves by concentrated external energy sources requires integration of the Euler equations (10)–(12) with boundary conditions defined in (16), (21), and (22). Besides the value of j defining the geometry and the specific-heat ratio γ of the gas, the solution depends on the heating rate $q(t)$, with the constant-heating-rate law (23) used in the computations shown below. For numerical purposes, it is advantageous to use the conservation equations written in the alternative characteristic form (13)–(15) and employ the transformed radial variable $(r - r_e)/(r_d - r_e)$. First-order finite differences were used in the integration, with up to 5000 cell points in the radial discretization. An implicit scheme was used, with time steps ranging from $\delta t = 10^{-6}$ for $t \ll 1$ to $\delta t = 10^{-5}$ for larger times and with the number of iterations at each time step being as large as 20 for small times. The characteristic equations C^- and C^0 were integrated from $r = r_d$, whereas implicit central differences were used for the characteristic equations C^+. This scheme enables the transition to CJ to be described for cylindrical and spherical detonations, as explained below.

3. Direct initiation of divergent detonations

As previously mentioned, the evolution of the initiation solution for spherical and axisymmetric configurations is similar, but quite different from that found in the planar case, which is treated separately below. As an illustrative example, we show in Figs. 2–4 results of computations corresponding to a line source with $t_d = 0.1$ and $\gamma = 1.4$. Fig. 2 shows the variation with time of the two fronts r_e and r_d and their velocities $\dot{r}_e$ and D. As can be seen, the detonation velocity decreases continuously, due to the expansion waves and the flow divergence, until it reaches the CJ velocity $D = 1$ at $t = t_c = 1.767$ when $r_d = r_c = 2.071$. The piston-like contact surface r_e keeps moving outwards to reach a final radius for $t \gg 1$. It can be seen that $\ddot{r}_e$ changes abruptly when heat deposition ceases at $t = t_d = 0.1$, in agreement with (24), and that this sudden deceleration is felt at a later instant $t \simeq 0.18$ by the propagating detonation front, when reached by the expansion wave leaving the contact surface at $t = t_d$.

The evolution of the accompanying profiles of pressure and velocity is shown in Fig. 3, along with the profiles of p/ρ, which are proportional to the temperature T' according to the equation of state $T' = (D'^2_{\mathrm{CJ}}/R_g)(p/\rho)$. Note in this figure the gradual variation of the gradients of the flow variables behind the detonation front for $t < t_c$, as well as the appearance of infinite values of these gradients for $t > t_c$. The presence of the high-temperature core with constant pressure for $0 < r < r_e$, associated with the finite deposition time, is clearly visible in the profiles.

The pattern of characteristics corresponding to the computation of Figs. 2 and 3 is given in Fig. 4. Of the three characteristics of the Euler equations for these flows with central symmetry, two, namely C^0 and C^-, leave always the detonation front toward the burnt gases, while the third, the acoustic wave C^+, moving with velocity $v + a > D$, reaches the detonation from inside for $t \leqslant t_c$, when the detonation is overdriven. These expansion waves, together with the flow divergence effects,

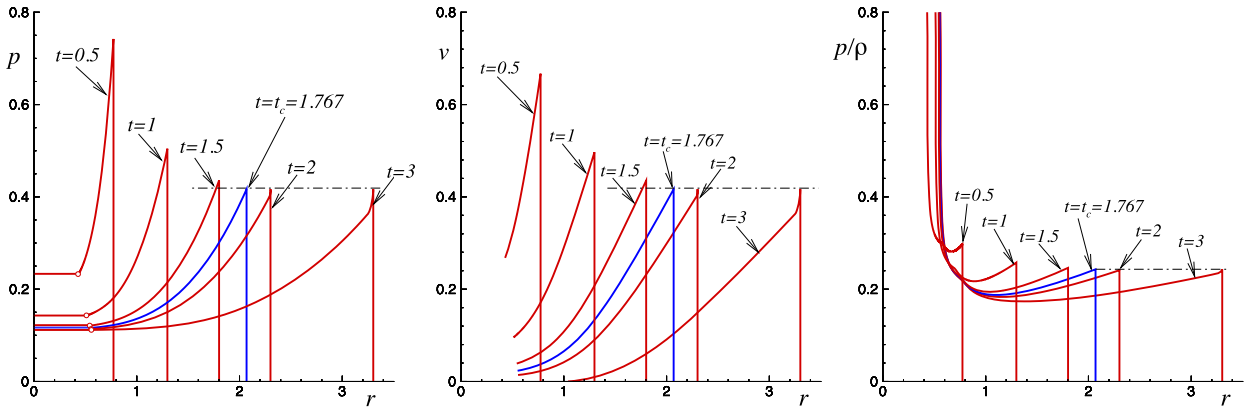

Fig. 3. Profiles of v, p, and p/ρ at different instants of time for $t_d = 0.1$, $\gamma = 1.4$ and $j = 1$.

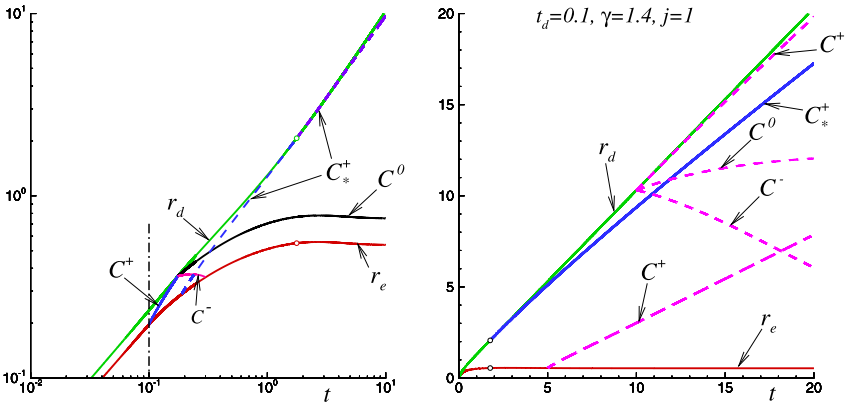

Fig. 4. The pattern of characteristics for $t_d = 0.1$, $\gamma = 1.4$ and $j = 1$, with logarithmic scales employed in the left-hand side plot to better expose the early evolution.

are responsible for the continuous deceleration of the detonation. In particular, the plot shows the characteristic C^+ leaving the contact surface at $t = t_d$, which reaches the detonation front at $t \simeq 0.18$, causing the detonation-front deceleration observed in Fig. 2. The relative slope $dr_*^+/dt - D$ with which C^+ intersects the front trajectory $r_d(t)$ decreases as the CJ point is approached, vanishing at $t = t_c$, so that the critical characteristic $C^+ = C_*^+$ reaching – and also leaving – the front at $t = t_c$ is tangent to the front trajectory $r_d(t)$, with $dr_*^+/dt = v + a = 1$ equal to the CJ detonation velocity $D = 1$. For $t > t_c$ all three characteristics depart from the detonation front, as can be observed in the right-hand side plot of Fig. 4. Since no C^+ characteristic can reach the front for $t > t_c$, the locus $r_*^+(t)$ of the critical characteristic C_*^+ defines for $t > t_c$ the inner boundary of a shell of gas $r_*^+ < r < r_d$ whose solution is independent of the flow found inside. The solution in the shell corresponds, exactly, to the ZT solution, and can be determined, for $t > t_c$, by integrating along the three characteristics leaving the detonation front $r_d = r_c + t - t_c$, where $\rho_d = \rho_{CJ} = (\gamma + 1)/\gamma$, $p_d = p_{CJ} = 1/(\gamma + 1)$, and $v_d = v_{CJ} = 1/(\gamma + 1)$; with the family of C^+ characteristics being tangent to the detonation locus. The associated profiles of pressure, density, and velocity coincide with those shown in Fig. 1 for the ZT solution, with ξ replaced by $r/(r_c + t - t_c)$ as long as $r > r_*^+$, the location of a weak discontinuity.

Because of the use of implicit central differences for the characteristic equations C^+, the numerical scheme appropriately handles the changes occurring at $t = t_c$, enabling the precise computation of r_c and t_c to be performed and the integration to be extended naturally for $t > t_c$, including the long-time evolution towards the ZT solution. The resulting values of r_c are shown in Fig. 5 as a function of t_d for two different values of γ. The numerical values of r_c determined here for $t_d \ll 1$ are seen to agree well with those reported earlier for instantaneous heat release [15], although small departures are noted, possibly attributable to the lower accuracy of the previous numerical scheme. For instance, for $\gamma = 1.4$ our computations give for $t_d \ll 1$ the values $r_c = (2.071, 1.32)$ for cylindrical and spherical detonations, whereas the results reported by Korobeinikov and Markov, expressed in the present notation, are $r_c = (1.93, 1.28)$.

As can be seen in Fig. 5, below a given value $t_d = t_d^*$ the resulting r_c shows a weak dependence on the deposition time t_d, whereas the value of r_c undergoes a pronounced drop for $t_d > t_d^*$. To understand this behavior, note that, as can be seen in the left-hand side plot of Fig. 4, the limiting characteristic $C^+ = C_*^+$ reaching the detonation at $t = t_c$ leaves the contact surface at an earlier time (e.g., $t \simeq 0.21$ for the conditions of Fig. 4), with the characteristics C^+ leaving the contact surface at later times never reaching the detonation. There exists a limiting case, corresponding precisely to deposition times

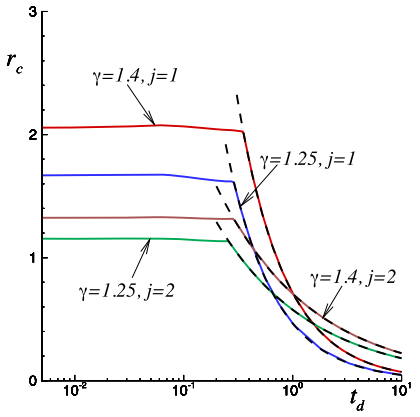

Fig. 5. The variation with t_d for the critical transition radius of cylindrical ($j=1$) and spherical ($j=2$) detonations for different values of γ.

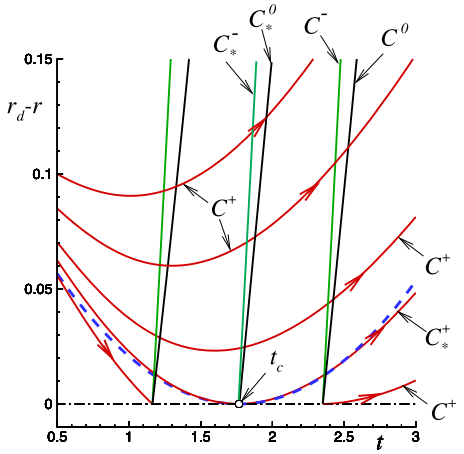

Fig. 6. A magnified view of Fig. 4 showing in detail the near-front pattern of characteristics immediately before and after transition for $t_d=0.1$, $\gamma=1.4$, and $j=1$. The dashed line represents the asymptotic prediction given in (42) for the limiting characteristic.

$t_d=t_d^*$, for which the C_*^+ characteristic leaves the contact surface at the exact instant when the heat deposition ends. For value of $t_d>t_d^*$, the fraction of the energy released for $t_d^*<t<t_d$ is not useful in the creation of a self-propagating shell of detonated gas bounded outside by a CJ detonation front, which originates at $r=r_c$ at the time $t=t_c$; but affects the evolution of the gas inside the inner boundary $r=r_*^+(t)$ of the shell. Clearly, for an effective use of the energy released, detonation igniters should be designed with deposition times $t_d<t_d^*$.

4. The near-front flow field at times close to transition to CJ

We have seen how for divergent detonations the effect of curvature enables the transition to CJ to occur at a precise time t_c. An analytical description can be derived for the flow near the front as a local expansion for small values of the time $\tau=t-t_c$. The analysis includes a pre-transition stage for $\tau<0$, when the detonation front speed D has decayed to slightly overdriven values such that $0<D-1=\delta\ll 1$, with $\delta\sim\tau^2$ as we shall show below, and also a post-transition stage for $\tau>0$, when $D=1$. Due to the transonic character of the flow behind the front, the associated near-front variation of the flow variables is of order $\sqrt{\delta}$, as seen below in (25). Because of the abrupt change in the pattern of characteristics occurring near the front at transition, illustrated in the magnified view given in Fig. 6, separate analyses will be needed for the pre-transition and post-transition stages.

Close to transition the flow is nearly sonic with respect to the detonation front and the properties immediately behind the detonation differ by a small amount from their corresponding CJ values, given in (19) and (20). The simplified expressions

$$\begin{cases} p_d/p_{\mathrm{CJ}}=1+\sqrt{2\delta}+2\delta \\ v_d/v_{\mathrm{CJ}}=1+\sqrt{2\delta}+\delta \\ \rho_{\mathrm{CJ}}/\rho_d=1-\sqrt{2\delta}/\gamma \\ a_d/a_{\mathrm{CJ}}=1+\sqrt{2\delta}(\gamma-1)/(2\gamma)+\delta(\gamma-1)(3\gamma+1)/\left(4\gamma^2\right) \end{cases} \tag{25}$$

are obtained from (17) and (18) when terms of order $\delta^{3/2}$ are neglected. While the departures of the pressure, density, velocity and sound velocity from their CJ values are seen to be of order $\sqrt{\delta}$ due to the transonic character of the flow, the variations of entropy, determined in the first approximation by

$$\frac{s-s_{\mathrm{CJ}}}{c_v}=\ln\left(\frac{p_d/p_{\mathrm{CJ}}}{(\rho_d/\rho_{\mathrm{CJ}})^{\gamma}}\right)=\frac{\gamma-1}{\gamma}\delta \tag{26}$$

are only of order δ. For $t>t_c$ the velocity is $\delta=0$ and one recovers from (25) the CJ values behind the detonation.

To obtain the solution for $t<t_c$, we rewrite the characteristic equations (13)–(15) for the perturbed variables

$$\tilde{v}=v-v_{\mathrm{CJ}},\qquad \tilde{a}=a-a_{\mathrm{CJ}}\quad\text{and}\quad \tilde{s}=s-s_{\mathrm{CJ}} \tag{27}$$

with use made of the normalized independent variables

$$\tau=\frac{t-t_c}{r_c}\ll 1\quad\text{and}\quad \eta=\frac{r-r_d}{r_c}\ll 1 \tag{28}$$

where r_c and t_c are the values of r_d and t at the transition time, given by the numerical solution as a function of t_d and γ. Keeping only the dominant terms in (13)–(15) yields

$$\frac{\partial}{\partial\tau}\left(\tilde{v}+\frac{2}{\gamma-1}\tilde{a}\right)+(\tilde{v}+\tilde{a})\frac{\partial}{\partial\eta}\left(\tilde{v}+\frac{2}{\gamma-1}\tilde{a}\right)-\frac{a_{\mathrm{CJ}}^2}{\gamma(\gamma-1)}\frac{\partial}{\partial\eta}\left(\frac{\tilde{s}}{c_v}\right)+jv_{\mathrm{CJ}}a_{\mathrm{CJ}}\frac{r_c}{r_d}=0 \tag{29}$$

$$\frac{\partial}{\partial\tau}\left(\tilde{v}-\frac{2}{\gamma-1}\tilde{a}\right)-2a_{\mathrm{CJ}}\frac{\partial}{\partial\eta}\left(\tilde{v}-\frac{2}{\gamma-1}\tilde{a}\right)-\frac{a_{\mathrm{CJ}}^2}{\gamma(\gamma-1)}\frac{\partial}{\partial\eta}\left(\frac{\tilde{s}}{c_v}\right)-jv_{\mathrm{CJ}}a_{\mathrm{CJ}}\frac{r_c}{r_d}=0 \tag{30}$$

$$\frac{\partial\tilde{s}}{\partial\tau}-a_{\mathrm{CJ}}\frac{\partial\tilde{s}}{\partial\eta}=0 \tag{31}$$

where $\mathrm{d}r_d/\mathrm{d}t=1+\delta$ and $a_{\mathrm{CJ}}=1-v_{\mathrm{CJ}}=\gamma/(\gamma+1)$. The associated boundary conditions, at $\eta=0$, for the leading terms,

$$\tilde{v}=\frac{1}{\gamma+1}\sqrt{2\delta},\qquad \tilde{a}=\frac{(\gamma-1)}{2(\gamma+1)}\sqrt{2\delta},\quad\text{and}\quad \frac{\tilde{s}}{c_v}=\frac{\gamma-1}{\gamma}\delta \tag{32}$$

readily follow from (25) and (26), which give, up to terms of order δ,

$$J^{\pm}=\tilde{v}_d\pm\frac{2}{\gamma-1}\tilde{a}_d=\sqrt{2\delta}\left(\frac{1}{\gamma+1}\pm\frac{1}{\gamma+1}\right)+\delta\left(\frac{1}{\gamma+1}\pm\frac{3\gamma+1}{2\gamma^2}\right) \tag{33}$$

for the boundary values of the Riemann invariants behind the detonation front.

An order-of-magnitude analysis of (29)–(31), based on the values $\tilde{v}\sim\tilde{a}\sim\delta^{1/2}$ and $\tilde{s}/c_v\sim\delta$ given by (32), serves to simplify the problem as follows. The last equation (31) provides $\partial(\tilde{s}/c_v)/\partial\eta\sim\delta/\tau$ for the entropy gradient in the transition region. This estimate can be used in (29) and (30) to show that the changes to the Riemann invariants associated with the nonuniform entropy field are negligible compared with the changes due to the unsteady and curvature effects, so that the resulting flow becomes effectively homentropic. The condition that the remaining three terms in (29) be comparable defines the thickness of the transonic layer

$$0<-\eta\sim\tau^2\sim\delta \tag{34}$$

where the outward propagating characteristics are interacting with the curved front. The changes in the second invariant, represented by the second term in (30), are of order τ^2 across the layer $-\eta\sim\tau^2$, because they are due to the first and last terms in this equation, both of order unity. As a result

$$\frac{\partial}{\partial\eta}\left(\tilde{v}-\frac{2\tilde{a}}{\gamma-1}\right)=0 \tag{35}$$

with relative errors of order $\delta^{1/2}$. Integrating (35) subject to $\tilde{v}-2\tilde{a}/(\gamma-1)=0$ at $\eta=0$ provides $\tilde{v}=2\tilde{a}/(\gamma-1)$, which can be used to write (29) in the alternative form

$$\frac{\partial\tilde{v}}{\partial\tau}+\frac{\gamma+1}{2}\tilde{v}\frac{\partial\tilde{v}}{\partial\eta}=-\frac{j\gamma}{2(\gamma+1)^2} \tag{36}$$

The problem therefore reduces to that of integrating (36) for $\eta<0$ with the boundary conditions

$$\eta=0:\quad\begin{cases}\tau<0:\quad \tilde{v}=\tilde{v}_d=\sqrt{2\delta}/(\gamma+1)\\ \tau>0:\quad \tilde{v}=0\end{cases} \tag{37}$$

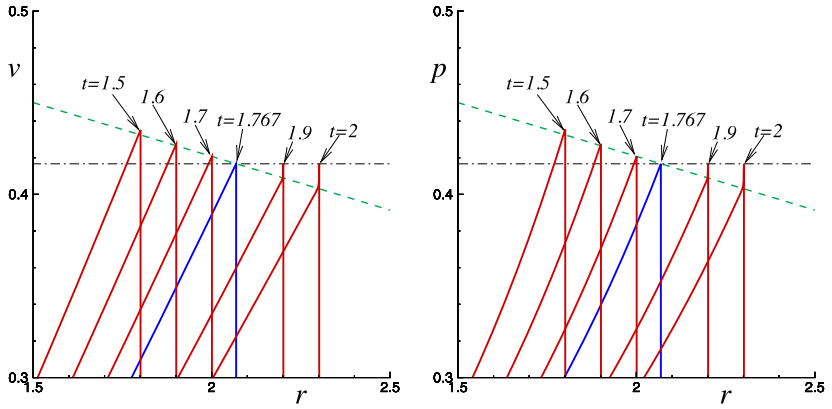

Fig. 7. A magnified view of Fig. 3 showing the evolution of the pressure and velocity profiles immediately before and after transition for $t_d = 0.1$, $\gamma = 1.4$, and $j = 1$; the dashed lines represent the asymptotic result (43).

For the numerical integration of (36) at $\tau < 0$, an initial condition $\tilde{v} = \tilde{v}_{d1} + A_1\eta$ should be added at $\tau = \tau_1 < 0$, where τ_1 must be small enough for $\tilde{v}_{d1} \ll 1$. Then, the velocity gradient $A_1 \sim O(1)$ will differ by a small amount from the velocity gradient A at $\tau = 0$, whose value is a function of t_d to be determined by numerical integration of the initiation problem. Separate consideration must be given to the solutions emerging before and after transition. We shall see below in (54) that the divergence-free version of (36) applies also for the description of the flow behind planar detonations when their propagation velocity differs by a small amount from the CJ value.

For $\tau < 0$, the gradient $\partial\tilde{v}/\partial\eta = A$ is imposed by the outer flow. As a result, the second term in (36), associated with the expansion waves reaching the front from inside, becomes negligible, so that curvature controls the velocity evolution as transition is approached, yielding

$$\tilde{v} = \frac{2\tilde{a}}{\gamma - 1} = -J\tau + A\eta \tag{38}$$

upon integration, where

$$J = \frac{j\gamma}{2(\gamma+1)^2} \sim O(1) \quad \text{and} \quad A\eta \sim \tau^2 \tag{39}$$

At $\eta = 0$, $\tilde{v} = \tilde{v}_d = \sqrt{2\delta}/(\gamma+1)$, so that use of (38) yields

$$\delta = \left(\frac{j\gamma}{2(\gamma+1)}\right)^2 \frac{\tau^2}{2} = \left(\frac{j\gamma}{8(\gamma+1)}\right)^2 \left(\frac{t' - t'_c}{r'_c/D_{\mathrm{CJ}}}\right)^2 \tag{40}$$

for the front velocity. On the other hand, the C^+ characteristics are obtained from integrating

$$\frac{\mathrm{d}\eta^+}{\mathrm{d}\tau} = \frac{\gamma+1}{2}\tilde{v} \tag{41}$$

giving in general $\eta^+ = -(j\gamma\tau^2)/[8(\gamma+1)] + C_1$, where the constant C_1 is positive for the characteristics reaching the detonation for $\tau < 0$. Correspondingly, the limiting characteristic, which becomes a weak discontinuity for $\tau > 0$, is given by

$$\eta^+_* = -\frac{j\gamma}{8(\gamma+1)}\tau^2 \tag{42}$$

The velocity and pressure along this limiting characteristic, given in the first approximation by

$$v - v_{\mathrm{CJ}} = p - p_{\mathrm{CJ}} = -\frac{j\gamma}{2(\gamma+1)^2}\frac{r - r_c}{r_c} \tag{43}$$

are plotted along with the numerical results in the detailed profile view of Fig. 7.

An interesting result concerning the direct initiation of divergent detonations is that, although the initial decay of D for $D - 1 \sim O(1)$ is the result of the combined effects of the expansion waves, reaching the overdriven detonation from inside, and of the flow divergence, only the latter controls the final evolution at transition, giving a universal velocity decay law

$$\frac{\partial\tilde{v}}{\partial t} = -\frac{j\gamma}{2(\gamma+1)^2 r_c} \tag{44}$$

which depends only on curvature effects.

By way of contrast, the velocity $\tilde{v}$ is still given by (36) for $\tau > 0$ in the intermediate region $0 > \eta > \eta_*^+$ extending between the detonation and the limiting characteristic. The solution, which is self-similar, can be described in terms of the normalized variables $\Lambda = \eta/\eta_*^+$ and $V = \tilde{v}/(-J\tau)$, reducing the problem to that of integrating

$$V - 2\Lambda\frac{dV}{d\Lambda} + 2V\frac{dV}{d\Lambda} = 1; \quad V = 0 \text{ at } \Lambda = 0 \tag{45}$$

The solution $V = \sqrt{\Lambda}$, readily obtained by inspection, provides

$$\frac{\tilde{v}}{\tau} = -\frac{j\gamma}{2(\gamma+1)^2}\left(\frac{\eta}{\eta_*^+}\right)^{1/2} \tag{46}$$

when written in terms of the near-front original variables. This velocity profile for the self-propagating shell, $\eta_*^+ < \eta < 0$, corresponds exactly to the profiles given by the ZT self-similar solution with the apparent origin at $r = 0$ and $t = -(r_c - t_c)$.

5. Direct initiation of planar detonations

As previously mentioned, in the limit of infinitely fast chemical reaction treated here the detonation front initiated by heat release at a plane decays continuously to approach the CJ solution only asymptotically for large times. The solution is described below for heat sources of constant heating rate and finite nonzero deposition times.

During the deposition period the solution is self-similar, with uniform constant values of the velocity and pressure between the contact surface and the detonation front, which moves at constant velocity $\bar{D}$. With constant uniform pressure, the condition (22) reduces to

$$\bar{p}_e\frac{dr_e}{dt} = \frac{\gamma-1}{2\gamma t_d} \tag{47}$$

where the inner-core pressure $\bar{p}_e$ is equal to the pressure behind the detonation, $\bar{p}_d$, given by (18), so that

$$\bar{p}_e = \bar{p}_d = \frac{\bar{D}^2}{\gamma+1}\left[1 + \left(1 - \bar{D}^{-2}\right)^{1/2}\right] \tag{48}$$

for an overdriven detonation, while the contact-surface velocity is determined from (21) by using the condition of uniform velocity $\bar{v} = \bar{v}_d = \bar{v}_e$ together with (17) to give

$$\bar{v}_e = \frac{dr_e}{dt} = \frac{\bar{D}}{\gamma+1}\left[1 + \left(1 - \bar{D}^{-2}\right)^{1/2}\right] \tag{49}$$

In the formulation bars will be used to denote the constant properties found during the self-similar deposition period. Substituting now (48) and (49) into (47) yields

$$\frac{2\gamma}{(\gamma-1)}\frac{\bar{D}^3[1 + (1 - \bar{D}^{-2})^{1/2}]^2}{(\gamma+1)^2} = t_d^{-1} \tag{50}$$

as an equation linking the detonation-front velocity during the deposition period with the deposition time t_d. It has solutions for values of t_d not larger than a critical value $t_d = t_{d_c}$ given by

$$t_{d_c} = \frac{(\gamma-1)(\gamma+1)^2}{2\gamma} \tag{51}$$

for which $\bar{D} = 1$, and the CJ velocity is already reached during the heating period and maintained afterwards; notice that $t_{d_c} \simeq 0.823$ for $\gamma = 1.4$. The solutions for $t_d > t_{d_c}$, similar to those found in the piston-supported detonations analyzed by Sedov [20] and Lee et al. [21], include an internal shock wave separating the inner uniform flow from an outer region described by the ZT solution. However, these solutions are not relevant for the problem of initiation of the CJ detonation, and will not be considered in the following.

The solution ceases to be self-similar for $t > t_d$ and requires in general numerical integration of (13)–(15) written for $j = 0$, with the condition (22) written in the simplified form

$$p_e r_e^\gamma = \bar{p}_e \bar{r}_e^\gamma \tag{52}$$

in terms of the initial contact-surface location $r_e = \bar{r}_e = \bar{v}_e t_d$ at $t = t_d$. Results of numerical integrations are shown in Figs. 8 and 9. The case $t_{d_c} - t_d \ll 1$, corresponding to slightly overdriven detonations with propagation velocities $D - 1 = \delta \ll 1$, admits a simplified analytical description, presented in Appendix A.

As seen in Fig. 8, the detonation velocity decays continuously in time towards the CJ value as the contact surface decelerates to rest and the solution approaches the ZT solution given in (6), which is plotted along with the velocity profiles in

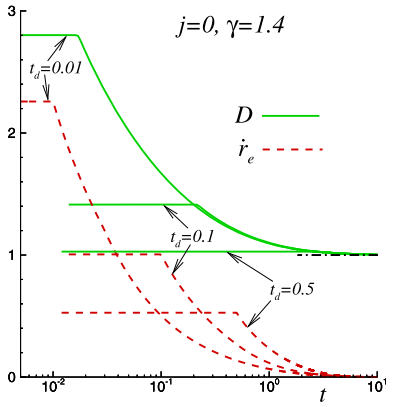

Fig. 8. The evolution with time of the detonation and contact-surface velocity for the planar detonation.

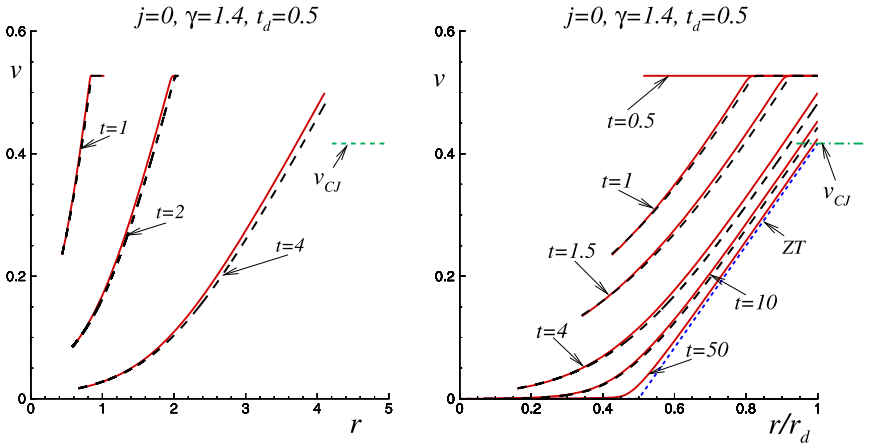

Fig. 9. The evolution with time of the velocity profiles behind the planar detonation with $\gamma = 1.4$ as obtained form numerical integration for $t_d = 0.5$ (solid curves). The dashed curves represent the ZT solution approached for $t \gg 1$ and the simplified profiles obtained by integrating (54) as indicated in Appendix A.

Fig. 9. The numerical results in Fig. 8 indicate that the decay of D towards $D = 1$ is very fast, so that values $D - 1 < 0.1$ are found already for $t = 2$. As seen above in (26), for this near-CJ evolution stage the entropy variations are of order $D - 1 = \delta$, much smaller than the variations of the other flow variables. At leading order, the resulting flow is homentropic, with small entropy gradients that can be neglected in (13) and (14). Small errors of order δ are also neglected in evaluating from (33) the Riemann invariant $J^- = v - 2a/(\gamma - 1)$ behind the detonation front, giving the constant value $J^- = v_{\mathrm{CJ}} - 2a_{\mathrm{CJ}}/(\gamma - 1)$, so that integration of (14) with boundary conditions at $r = r_d$ yields

$$v - \frac{2a}{\gamma - 1} = v_{\mathrm{CJ}} - \frac{2a_{\mathrm{CJ}}}{\gamma - 1} \tag{53}$$

up to terms of order $\sqrt{\delta}$. Using this result in (13) and introducing a coordinate $\zeta = r - r_d$ and a near-front velocity $\tilde{v} = v - v_{\mathrm{CJ}}$ leads to

$$\frac{\partial \tilde{v}}{\partial t} + \frac{\gamma + 1}{2}\tilde{v}\frac{\partial \tilde{v}}{\partial \zeta} = 0 \tag{54}$$

for the evolution of the velocity, which is identical to the divergence-free version, for $j = 0$, of (36).

The evolution of the detonation front and the flow field near the front can be described using (54) with the boundary condition $\tilde{v} = \tilde{v}_d = \sqrt{2\delta}/(\gamma + 1)$ at $\zeta = 0$ and an initial condition at a time $t = t_1$ moderately larger than one, to ensure that $\tilde{v}_d = \tilde{v}_{d1} \ll 1$. The initial velocity profile for sufficiently small values of ζ, such that $\tilde{v} > 0$, can be approximated by the linear profile $\tilde{v} = \tilde{v}_{d1} + A_1\zeta$; where $A_1 \sim O(1)$ as well as $\tilde{v}_{d1}$ must be obtained from the numerical solution in terms of t_d.

Eq. (54) shows that $\tilde{v}$ is constant along the characteristics, which are straight lines departing from $\zeta = \lambda$ at $t = t_1$, so that

$$\tilde{v} = \tilde{v}_{d1} + A_1\lambda \quad \text{at } \zeta = \lambda + (\tilde{v}_{d1} + A_1\lambda)\frac{\gamma + 1}{2}(t - t_1) \tag{55}$$

Note that the characteristic leaving from $\zeta = \zeta_1 = -\tilde{v}_{d1}/A_1$ corresponds to a velocity $\tilde{v} = \tilde{v}_{d1} + A_1\zeta = 0$, and therefore remains parallel to the detonation front, never reaching it. The velocity behind the detonation is therefore determined by the characteristics corresponding to $\zeta_1 < \lambda < 0$. The flow velocity at the front $\tilde{v}_d$ is obtained by considering the characteristic that reaches $\zeta = 0$ at time t,

$$0 = \lambda + (\tilde{v}_{d1} + A_1\lambda)\frac{\gamma+1}{2}(t - t_1) \tag{56}$$

which imposes a velocity given by

$$\tilde{v}_d = \tilde{v}_{d1} + A_1\lambda \tag{57}$$

Eliminating λ from (56) and (57) yields

$$\tilde{v}_d = \frac{\tilde{v}_{d1}}{1 + A_1(\gamma+1)(t-t_1)/2} \tag{58}$$

which further reduces to

$$\tilde{v}_d = \frac{2}{\gamma+1}\frac{\tilde{v}_{d1}/A_1}{t} = \frac{2}{\gamma+1}\frac{-\zeta_1}{t} \tag{59}$$

for $t - t_1 \gg 1$. Since the velocity must vanish at the limiting characteristic $\zeta = \zeta_1$, the corresponding linear velocity distribution is

$$\tilde{v} = \frac{2}{\gamma+1}\frac{\zeta - \zeta_1}{t} \tag{60}$$

whose slope naturally takes the ZT value $\partial\tilde{v}/\partial\zeta = 2/[(\gamma+1)t]$ given in (6). Note also that the Rankine–Hugoniot condition $\tilde{v}_d = \sqrt{2\delta}/(\gamma+1)$ can be used together with (59) to give

$$\delta = \frac{2\zeta_1^2}{t^2} \tag{61}$$

for the long-time decay of the planar detonation front velocity. In general, the value of ζ_1 must be determined numerically. As shown in Appendix A, for heating sources with deposition times t_d close to the critical value t_{d_c}, the resulting value is $\zeta_1 = -(\gamma^2 - 1)/2$.

6. Concluding remarks

The study presented in this paper deals with the initiation of self-sustained detonations by, spatially concentrated, external energy sources of finite deposition time. It provides the outer flow structure for fast chemical reactions when the thickness of the reaction layer is considered to be small compared with the radius of the detonation.

The inner structure of the reaction layer has been described, using the quasi-steady approximation, by He and Clavin [6], with results for the minimum initiating energy that compare favorably with numerical results, presented also in [6]. It is interesting to observe that their numerical results show that the thickness of the reaction layer is two orders of magnitude smaller than the shock radius for supercritical energy sources, and also for the subcritical cases before splitting occurs between the flame zone and leading shock wave due to finite-rate effects. The improved understanding of the flow structure near the detonation front, presented here, will help us to ascertain the reasons for the accuracy of the quasi-steady reaction-layer prediction of the minimum energy given by He and Clavin [6]. We also believe that our paper will provide indications on how to account for unsteady effects in the reaction-layer analysis.

The paper includes in Section 5 a description of the direct initiation of planar detonations by external energy deposition, with constant rate, during a time t_d. During the deposition period a hot slab is pushing, as a piston with constant velocity, the detonation products, whose flow properties as well as the detonation velocity remain constant. These properties change in a nonsimilar form for $t > t_d$, described numerically for $t - t_d \sim O(1)$ and analytically for large values of t, when the detonation-front velocity approaches its CJ value. The case when t_d is moderately close to t_{d_c}, when $D - 1 = \delta \ll 1$ for all times, is amenable to the analytical treatment given in Appendix A.

The asymptotic analysis for large time presented in this study for $j = 0$ leads to results that were anticipated by Levin and Chernyi [17] in their asymptotic analysis of the planar case, also based on the assumption that at leading order the flow field near the front is at large times homentropic and with a constant value of the J^- invariant; so they can conclude that the resulting flow corresponds to a Riemann wave.

Our analysis includes the Burger-like equation (54), which for planar detonations governs the transonic velocity field for large times. This equation should be generalized to account for finite-rate effects and for the curvature effects associated with the transverse perturbations in a nonlinear analysis of instability of near-planar detonation fronts, as hinted by (44).

Acknowledgements

We thank Paul Clavin for his insight into this problem and for numerous fruitful scientific conversations over many years. The senior author had the privilege of meeting Paul Clavin and his PhD student Guy Joulin at the meeting in Bourges in 1975. Both showed plainly an unlimited curiosity and interest in the fundamentals of combustion science. This first meeting was followed very soon by a deep friendship and a most fruitful collaboration that, in an unmeasurable way, has enriched the senior author's life and his work, often made more relevant after many enjoyable discussions with Paul Clavin. This work was supported by the Spanish MCINN through the Program CONSOLIDER-Ingenio 2010 (project # CSD2010-00011).

Appendix A. Initiation of planar detonations for near-critical conditions

The initiation of a planar detonation by a concentrated source of constant heating rate admits a simplified description when the deposition time is close to the critical value, i.e., $t_{d_c} - t_d \ll 1$. For these near-critical conditions, the detonation is weakly overdriven during the deposition stage, with velocities $\bar{D} - 1 = \bar{\delta} \ll 1$ such that

$$\bar{\delta} \simeq \frac{1}{8}(t_{d_c}/t_d - 1)^2 \tag{62}$$

as follows from (50) and (51), and pressures and velocities

$$\frac{\bar{p}_e}{p_{\mathrm{CJ}}} = \frac{\bar{p}_d}{p_{\mathrm{CJ}}} = \frac{\bar{v}_e}{v_{\mathrm{CJ}}} = \frac{\bar{v}_d}{v_{\mathrm{CJ}}} \simeq 1 + \sqrt{2\bar{\delta}} \tag{63}$$

given by (48) and (49).

For $t > t_d$, the detonation propagation velocity $\delta(t)$ decays from the initial value $\delta = \bar{\delta} \ll 1$ to approach $\delta = 0$ for $t \to \infty$, while the contact surface, moving initially at constant velocity

$$\frac{\mathrm{d}r_e}{\mathrm{d}t} \simeq \frac{1 + \sqrt{2\bar{\delta}}}{\gamma + 1} \tag{64}$$

as can be obtained from (49), decelerates to rest. According to the discussion in the previous paragraph, since $\delta(t)$ is always small, the flow is homentropic in the first approximation and the flow field is everywhere determined by (53) and (54). The evolution of the contact-surface radius from its initial value

$$\bar{r}_e \simeq \frac{1 + \sqrt{2\bar{\delta}}}{\gamma + 1} t_d \simeq \frac{\gamma^2 - 1}{2\gamma}(1 - \sqrt{2\bar{\delta}}) \tag{65}$$

can be computed by integrating (21), with the contact-surface velocity

$$\frac{v_e}{v_{\mathrm{CJ}}} = 1 + \frac{2\gamma}{\gamma - 1}\left(\frac{a_e}{a_{\mathrm{CJ}}} - 1\right) \tag{66}$$

determined from (53) in terms of

$$\frac{a_e}{a_{\mathrm{CJ}}} = \left(\frac{\bar{p}_e}{p_{\mathrm{CJ}}}\right)^{(\gamma-1)/(2\gamma)} \left(\frac{\bar{r}_e}{r_e}\right)^{(\gamma-1)/2} \tag{67}$$

which is expressed here with use made of (52) and of the condition of homentropic flow

$$\left(\frac{p_e}{p_{\mathrm{CJ}}}\right)^{(\gamma-1)/\gamma} = \left(\frac{a_e}{a_{\mathrm{CJ}}}\right)^2 \tag{68}$$

The problem reduces to that of integrating

$$\frac{\mathrm{d}r_e}{\mathrm{d}t} = -\frac{1}{\gamma - 1} + \frac{2\gamma}{\gamma^2 - 1}\left(\frac{\bar{p}_e}{p_{\mathrm{CJ}}}\right)^{(\gamma-1)/(2\gamma)} \left(\frac{\bar{r}_e}{r_e}\right)^{(\gamma-1)/2} \tag{69}$$

with initial condition $r_e = \bar{r}_e$ at $t = t_d$ to give

$$\int_1^{r_e/\bar{r}_e} \frac{\mathrm{d}X_e}{[1 + \frac{\gamma-1}{2\gamma}\sqrt{2\bar{\delta}}\,]X_e^{-(\gamma-1)/2} - \frac{\gamma+1}{2\gamma}} = \left(\frac{2\gamma}{\gamma^2 - 1}\right)^2 \frac{t - t_d}{1 - \sqrt{2\bar{\delta}}} \tag{70}$$

with errors of order $\bar{\delta}$. The result is compared in Fig. 10 with results of numerical integrations for different values of t_d. As can be seen, because of the square dependence present in (62), the resulting description becomes very accurate even for values of the deposition time relatively far from the critical value $t_{d_c} = 0.823$.

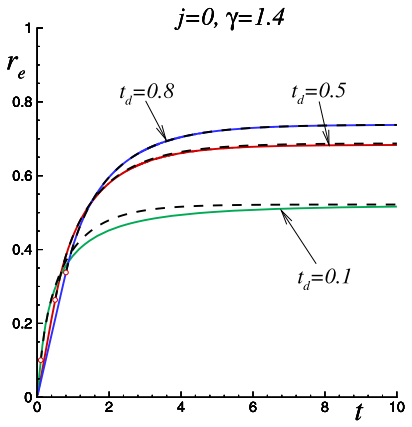

Fig. 10. The evolution with time of the contact-surface radius for the planar detonation as obtained form numerical integration (solid curves) and from (70) (dashed curves).

Once $r_e(t)$ is computed, the velocity field is obtained by integrating the C^+ characteristic equation (54) for $\zeta_e < \zeta < 0$ with boundary condition $v = \mathrm{d}r_e/\mathrm{d}t$ at $\zeta = \zeta_e$. In computing $\zeta_e = r_e - r_d < 0$, the boundary value $v = v_d$ at $\zeta = 0$ is used to determine the evolution of $r_d(t)$ according to

$$\frac{\mathrm{d}r_d}{\mathrm{d}t} = 1 + \frac{1}{2}\big[(\gamma+1)v_d - 1\big]^2 \tag{71}$$

obtained by solving the approximate equation $v_d = v_{\mathrm{CJ}}(1+\sqrt{2\delta})$. The resulting velocity profiles are in close agreement with those obtained from the complete integration, as can be seen in the comparisons of Fig. 9.

An approximate expression can be derived for the detonation velocity $\delta(t)$ by analyzing the interaction of the characteristics with the detonation front. The C^+ characteristics are straight lines departing from the contact surface with slope

$$\frac{\mathrm{d}r^+}{\mathrm{d}t} = v + a = 1 + \frac{\gamma+1}{2}(v - v_{\mathrm{CJ}}) \tag{72}$$

as can be obtained with use made of (53), with v corresponding to the contact-surface velocity $v_e = \mathrm{d}r_e/\mathrm{d}t$ at the departing point. Since the detonation velocity is close to unity, the condition $v = v_e > v_{\mathrm{CJ}}$ is necessary for a given characteristic to reach the detonation front. In the limit considered here, the contact-surface velocity has an initial value $\bar{v}_e = v_{\mathrm{CJ}}(1+\sqrt{2\bar{\delta}})$, only slightly above v_{CJ}, and decays towards zero reaching rapidly $v_e = v_{\mathrm{CJ}}$ for $t - t_d \sim \sqrt{\bar{\delta}}$. As a result, only the expansion waves generated after the heat source is turned off, that is, for $t - t_d \sim \sqrt{\bar{\delta}}$ when $r_e - \bar{r}_e \sim \sqrt{\bar{\delta}}$, are able to reach the detonation front and modify its velocity. In considering the characteristics interacting with the detonation, all leaving soon after $t = t_d$ and running almost parallel to the detonation front, we may therefore use for simplicity $r = \bar{r}_e$ and $t = t_d$ as their origin to write

$$\frac{r - \bar{r}_e}{t - t_d} = 1 + \frac{\gamma+1}{2}(v - v_{\mathrm{CJ}}) \tag{73}$$

The first characteristic reaches the front after a long period given in the first approximation by

$$t - t_d = \frac{2\gamma t_d}{\gamma+1}\frac{1}{\sqrt{2\bar{\delta}}} \tag{74}$$

as can be obtained from substituting into (73) the initial velocity $v = v_{\mathrm{CJ}}(1+\sqrt{2\bar{\delta}})$ along with the location of the detonation front $r = r_d = t$. Furthermore, Eq. (73) can be also used together with the detonation-front location $r = r_d = t$ to determine the flow velocity behind the detonation, yielding

$$v_d(t) = v_{\mathrm{CJ}}\left(1 + \frac{2\gamma}{\gamma+1}\frac{1}{t/t_d - 1}\right) \tag{75}$$

for $t/t_d - 1 > 2\gamma/[(\gamma+1)\sqrt{2\bar{\delta}}]$, whereas $v_d = \bar{v}_e = v_{\mathrm{CJ}}(1+\sqrt{2\bar{\delta}})$ for earlier times. Note that, since $t_d - t_{d_c} \ll 1$, with t_{d_c} given in (51), and $t \gg 1$, the above equation simplifies to give in the first approximation

$$v_d - v_{\mathrm{CJ}} = \frac{\gamma-1}{t} \quad \text{for } t > \frac{\gamma^2-1}{\sqrt{2\bar{\delta}}} \tag{76}$$

Using now the Rankine–Hugoniot condition $v_d = v_{CJ}(1+\sqrt{2\delta})$ provides

$$\delta = \frac{(\gamma^2-1)^2}{2t^2} \quad \text{for } t > \frac{\gamma^2-1}{\sqrt{2\delta}} \tag{77}$$

for the detonation velocity, in agreement with the general result given above in (61).

References

[1] Ya.B. Zel'dovich, On the theory of the propagation of detonations in gaseous systems, Zhurn. Eksper. Teor. Fiz. 10 (1940) 542–568.
[2] J. von Neumann, Theory of detonation waves, Prog. Rept. No. 238 (April 1942), O.S.R.D Rept. No. 549.
[3] W. Döring, On the detonation process in gases, Ann. Phys. 43 (1943) 421–436.
[4] V.P. Korobeinikov, Gas dynamics of explosions, Ann. Rev. Fluid Mech. 3 (1971) 317–346.
[5] Ya.B. Zel'dovich, S.M. Kogarko, N.N. Simonov, An experimental investigation of spherical detonation of gases, Sov. Phys. Tech. Phys. 1 (1956) 1689–1731.
[6] L. He, P. Clavin, On the direct initiation of gaseous detonations by an energy source, J. Fluid Mech. 277 (1994) 227–248.
[7] L.I. Sedov, Propagation of strong shock waves, J. Appl. Math. Mech. 10 (1946) 241–250.
[8] G.I. Taylor, The formation of a blast wave by a very intense explosion. I. Theoretical discussion, Proc. R. Soc. Lond. A 201 (1952) 159–174; II. The atomic explosion of 1945, Proc. R. Soc. Lond. A 201 (1952) 175–186.
[9] Ya.B. Zel'dovich, On the distribution of pressure and velocity in products of detonation blasts, in particular for spherically propagating detonation waves, Zhurn. Eksper. Teor. Fiz. 12 (1942) 389–406.
[10] G.I. Taylor, The dynamics of the combustion products behind plane and spherical detonation fronts in explosives, Proc. R. Soc. Lond. A 200 (1950) 235–247.
[11] E. Bishimov, Numerical solution of a problem of a strong point explosion in a detonating gas, in: Differential Equations and Their Applications, Nauka, Alma-Ata, 1968, pp. 94–103.
[12] V.P. Korobeinikov, The problem of point explosion in a detonating gas, Astronautica Acta 14 (1969) 411–419.
[13] W.H. Kyong, Numerical studies of gaseous detonation phenomena, Dissertation, McGill University, 1971.
[14] J.H.S. Lee, Gasdynamics of detonations, Astronautica Acta 17 (1972) 455–466.
[15] V.P. Korobeinikov, V.V. Markov, On the propagation of combustion and detonation, Arch. Thermodyn. Splan. Polska 8 (1977) 101–119.
[16] V.P. Korobeinikov, Problems of Point-Blast Theory, Nauka, Moscow, 1985.
[17] V.A. Levin, G.G. Chernyi, Asymptotic laws of behavior of detonation waves, Prikl. Mat. Mekh. 31 (1967) 393–405.
[18] G.G. Cherny, Lectures on the Theory of Exothermic Flows Behind Shock Waves, Springer Verlag, New York, 1973, pp. 35–38.
[19] V.N. Kurdyumov, A.L. Sánchez, A. Liñán, Heat propagation from an external energy source in a gas, J. Fluid Mech. 491 (2003) 379–410.
[20] L.I. Sedov, Similarity and Dimensional Methods in Mechanics, Academic Press, 1959.
[21] J.H.S. Lee, R. Knystautas, G.G. Bach, Theory of explosions, AFOSR Scientific Report 69-3090 TR, 1969.